

PCCP

Accepted Manuscript



This is an *Accepted Manuscript*, which has been through the Royal Society of Chemistry peer review process and has been accepted for publication.

Accepted Manuscripts are published online shortly after acceptance, before technical editing, formatting and proof reading. Using this free service, authors can make their results available to the community, in citable form, before we publish the edited article. We will replace this *Accepted Manuscript* with the edited and formatted *Advance Article* as soon as it is available.

You can find more information about *Accepted Manuscripts* in the [Information for Authors](#).

Please note that technical editing may introduce minor changes to the text and/or graphics, which may alter content. The journal's standard [Terms & Conditions](#) and the [Ethical guidelines](#) still apply. In no event shall the Royal Society of Chemistry be held responsible for any errors or omissions in this *Accepted Manuscript* or any consequences arising from the use of any information it contains.

2016 PCCP

Another challenge to paramagnetic relaxation theory: a study of paramagnetic proton NMR relaxation in closely related series of pyridine-derivatised dysprosium complexes [§]

Nicola J Rogers, Katie-Louise N. A. Finney, P. Kanthi Senanayake and David Parker *

^a Department of Chemistry, Durham University, South Road, Durham DH1 3LE, UK
email: david.parker@dur.ac.uk

Measurements of the relaxation rate behaviour of two series of dysprosium complexes have been performed in solution, over the field range 1.0 to 16.5 Tesla. The field dependence has been modelled using Bloch-Redfield-Wangsness theory, allowing estimates of the electronic relaxation time, T_{1e} , and the size of the magnetic susceptibility, μ_{eff} , to be made. Changes in relaxation rate of the order of 50% at higher fields were measured, following variation of the *para*-substituent in the single pyridine donor. The magnetic susceptibilities deviated unexpectedly from the free-ion values for certain derivatives in each series examined, in a manner that was independent of the electron-releasing/withdrawing ability of the pyridine substituent, suggesting that the polarisability of just one pyridine donor in octadenate ligands can play a significant role in defining the magnetic susceptibility anisotropy.

Introduction

The magnetic relaxation of coordination complexes of the paramagnetic lanthanide ions is usually considered using modifications of Bloch-Redfield-Wangsness (BRW) theory ¹. The paramagnetic relaxation arises from conformational and rotational modulation of the electron-nuclear dipolar interaction, eq. (1).

$$R_1 = \frac{2}{15} \left(\frac{\mu_0}{4\pi} \right)^2 \frac{\gamma_N^2 \mu_{\text{eff}}^2}{r^6} \left[\frac{7\tau_{R+e}}{1 + \omega_e^2 \tau_{R+e}^2} + \frac{3\tau_{R+e}}{1 + \omega_N^2 \tau_{R+e}^2} \right] + \frac{2}{5} \left(\frac{\mu_0}{4\pi} \right)^2 \frac{\omega_N^2 \mu_{\text{eff}}^4}{(3kT)^2 r^6} \frac{3\tau_R}{1 + \omega_N^2 \tau_R^2} \quad (1)$$

$$\mu_{\text{eff}}^2 = g_c^2 \mu_B^2 \langle \hat{S}^2 \rangle \quad \tau_{R+e} = (\tau_R^{-1} + T_{1e}^{-1})^{-1}$$

where μ_0 is the vacuum permeability, γ_N is the gyromagnetic ratio of the nucleus, g_{L_n} is the Landé factor of the fundamental multiplet J of the free Ln^{3+} ion, τ_r is the rotational correlation time in which isotropic tumbling is assumed, μ_B is the Bohr magneton (BM), r is the electron-nuclear distance, ω_N is the nuclear Larmor frequency, ω_e is the electron Larmor frequency and T_{1e} is the longitudinal relaxation time of the electron

2016 PCCP

spin. The dependence of R_1 on $(\mu_{\text{eff}})^4$ and $(\omega_N)^2$ in the Curie term (i.e. the second part of eq. 1) is more dominant at higher magnetic fields, especially for ions with large values of μ_{eff} . At high field, for systems that obey this theory, relaxation rates are predicted to echo the sequence of μ_{eff} values : Dy/Ho > Tb > Er > Tm > Yb. At lower fields (< 3 T), the rate of relaxation is determined primarily by electronic relaxation, T_{1e} , and the order can vary significantly.

One of the limitations of BRW theory is that the assumptions of perturbation theory for the electron are frequently violated, most notably the treatment of the induced electronic magnetisation as a point dipole. The analysis also requires information concerning several empirical parameters that are tricky to measure independently for a particular system, e.g. T_{1e} , τ_R and the true value of μ_{eff} . It has been suggested that the electronic relaxation time, T_{1e} , typically falling between 0.1 and 1 ps, is determined by the transient ligand field and the nature of the lanthanide ion, as the orbital contribution to the electronic levels facilitates an electronic relaxation mechanism via solvent collisions. In contrast to the behaviour of systems of low symmetry, the value of T_{1e} in systems with a C_3 or C_4 axis has been found to be directly proportional to the second-order ligand field term, B_0^2 .²

The effect of spin-orbit coupling on electronic energy levels in lanthanide ions is routinely assumed to be greater than the ligand field splitting that separates the J multiplets into m_J projections. Indeed, the Landé /van Vleck approximations used to treat lanthanide paramagnetism consider J to be a good quantum number, allowing experimental values of magnetic susceptibility for the 'free ions' to be calculated directly. These values are predicted to be independent of the coordination environment, i.e. not related to the ligand field. Spin-orbit coupling values range from 600 to 2000 cm^{-1} across the 4f series. However, values for the second order crystal field term, B_0^2 , can vary from near zero to as much as 1500 cm^{-1} ,⁴ and higher order crystal field terms may have even greater size, suggesting that the Landé and van Vleck approximations will not hold consistently.⁵ Even where J is a good quantum number, the ligand field splittings within a ground-state multiplet can be greater than kT at room temperature. In each case, the approximation that a room temperature magnetic moment can be derived from $|J|$ and the Landé factor g_J is not generally valid. Examples of lanthanide complexes with such large ligand fields are seldom studied in detail. However, Hölsä has shown that the room temperature magnetic moments are systematically lower than the free-ion values, notably for Ho(III), (-11%) using SQUID magnetometry in the LnOBr series, where values of B_0^2 vary from -1200 (Tb) to -1350 cm^{-1} (Yb).⁷

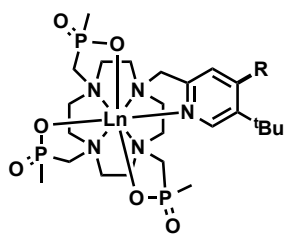
Lanthanide(III) ions possess different electron distributions in the 4f shell according to the nature of the ligand field. The electron density clouds for the biggest $|m_J|$ projections are

2016 PCCP

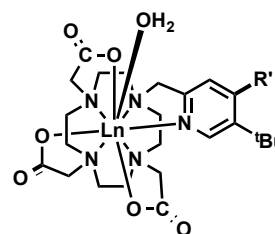
oblate for Ce, Tb, Pr, Dy, Nd and Ho and prolate for Yb, Tm, Er, Eu. The nature of a single axial substituent can cause a major change. Hence, ligand electron density on the molecular z axis can destabilise the maximum $|m_J|$ level for the latter ions and stabilise them for the oblate set.⁸ Thus, room temperature magnetic susceptibilities for Ln(III) ions in coordination complexes will change with coordination environment, especially in those situations where ligand field splittings are much bigger than kT .

Results and Discussion

Very recently, the importance of the anisotropy of the magnetic susceptibility in determining the NMR shift and relaxation behaviour of complexes of the fast-relaxing lanthanide(III) ions has been reaffirmed. Thus, in work examining the series of complexes with L^{1a} vs L^{2a} , ($R = H$: Ln = Tb, Dy, Ho, Er, Tm, Yb), the chemical shift of the reporter t -butyl group changes by over 50 ppm for the Tb, Tm and Dy complexes, and relaxation rates for Er and Tm were faster at low field than the Tb and Dy analogues.⁹⁻¹¹ Such chemical shift variations do not conform to Bleaney's theory of magnetic anisotropy, but can be rationalised by a major change in the relative size of the orthogonal components of the magnetic susceptibility tensor. Thus, the position of the principal magnetic axis may shift by 90° by a single ligand donor perturbation.¹²⁻¹⁴ Furthermore, the relaxation rate behaviour challenges the assumptions inherent in BRW theory.¹¹ In extending the work to closely related series of dysprosium complexes, a further test of the robustness of the current theory was set. Therefore in this work, two sets of dysprosium complexes, $[Dy.L^1]$ and $[Dy.L^2(H_2O)]$ have been examined and the impact of remote ligand substitution on spectral properties has been considered in two ways: the effect of varying the magnetic field on ligand 1H NMR longitudinal relaxation rate data^{2,10,11} R_1 has been measured, alongside emission spectral analyses in solution that provide information on changes in the ligand field. The two sets of Dy(III) complexes chosen for study were formed with closely related octadentate ligands based on 1,4,7,10-tetra-azacyclododecane (cyclen).

[Ln.L¹]

R = a) H; b) NMe₂; c) NO₂; d) CONH₂,
e) Cl; f) SCH₂CO₂; g) PO(OH)O-

[Ln.L²(H₂O)]

R = a) H; b) NHCOMe; c) NO₂
d) NMe₂; e) SCH₂CO₂-

The macrocyclic ligands are functionalized by three methylphosphinate, L^1 , or three

2016 PCCP

carboxylate groups, L^2 , with a common, coordinated pyridine ring. The substituent at the *para* position of the pyridine ring has been varied, and the series chosen provides examples of electron-withdrawing and electron-releasing groups, including charge neutral and anionic substituents.

Recent work has shown that the parent complexes of the tricarboxylate ligand possess one coordinated water molecule and are 9-coordinate, whereas analogous complexes of the triphosphinate series are octadentate with no coordinated water molecule.¹¹ The absence of the axial water molecule in the latter case is likely to affect the relative position and population of the $|m_J|$ sub-levels significantly, and hence is expected to change the relative size of the major components of the magnetic susceptibility tensor, as revealed by the preliminary NMR studies, and in accord with recent observations in related systems.¹²⁻¹⁴

Emission spectral analysis

The emission spectrum of each Dy(III) complex was recorded at 295 K in D_2O and at 200, 150 and 80 K in a MeOH/EtOH (4:1) frozen glass, following excitation into the pyridine $\pi-\pi^*$ transition around 270 nm. The pyridine group acts as an antenna and following intramolecular energy transfer from the pyridine triplet excited state, the lowest manifold of the $^4F_{9/2}$ excited state of the Dy(III) ion is populated. The main observed transitions occur to the $^6H_{15/2}$ and $^6H_{13/2}$ multiplets centred around 480 and 580 nm respectively. These transitions provide information on the nature of the ground and first excited state multiplets respectively.

The emission spectra obtained for each ligand set were identical, i.e. the spectral form observed was independent of the nature of the *para*-pyridine substituent, although large differences are observed between the tricarboxylate and triphosphinate series, notably at 295 K (Figure 1 and ESI). Comparative analysis of spectral data at 80 K ($kT = 56 \text{ cm}^{-1}$) and 295 K ($kT = 205 \text{ cm}^{-1}$) suggested that the bands at 494, 469, 460 and 589, 582.5 nm for $[Dy.L^{1a/1b}]$ were 'hot bands', (Table 1), associated with transitions from a higher energy component of the $^4F_{9/2}$ excited state manifold. Their relative intensity diminished with temperature in a parallel manner (ESI). The appearance of a hot band at the lowest energy for the phosphinate system is counter-intuitive, and suggests that one of the eight transitions from the lowest energy excited state component may be very weak and may not be observed here. Recent studies of Dy emission spectral analysis in 8 or 9 coordinate complexes have shown that the lowest two levels of the $^4F_{9/2}$ manifold are separated by about 40 to 60 cm^{-1} .^{12b,15,16} For $[Dy.L^2]$, the putative hot bands were not so well resolved, and variable temperature spectral analysis did not permit their identification (ESI).

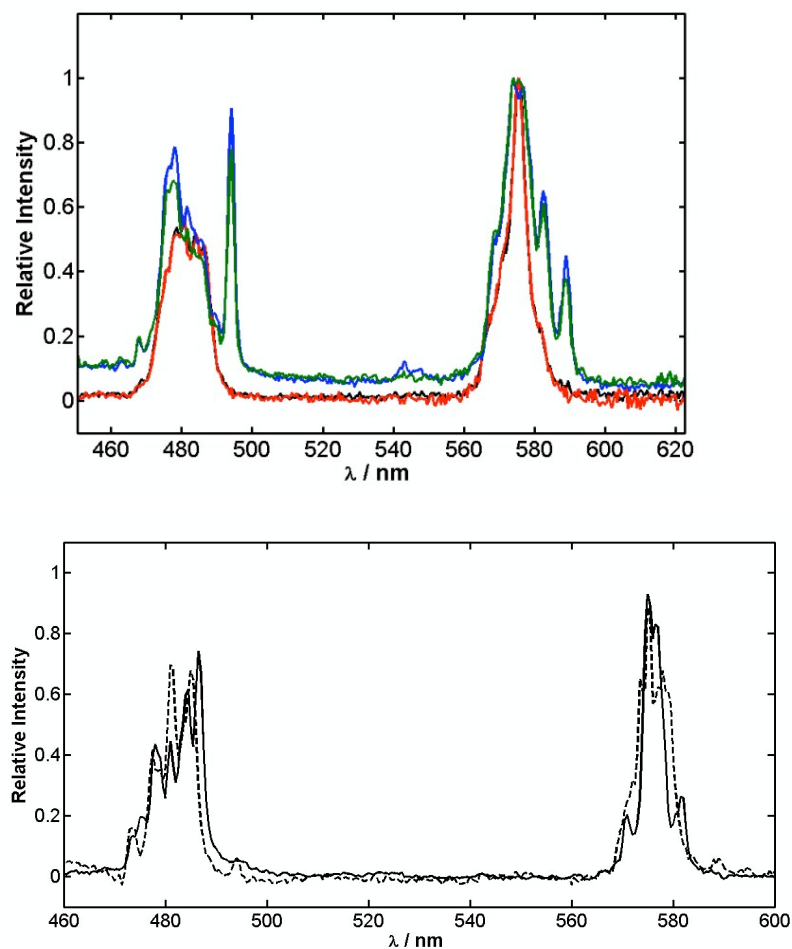


Figure 1 (upper) Partial solution emission spectra for [Dy.L^{1a}] (blue), [Dy.L^{1f}] (green), [Dy.L^{2a}(H₂O)] (black) and [Dy.L^{2d}(H₂O)] (red) showing the ⁴F_{9/2} - ⁶H_{15/2} (left) and ⁴F_{9/2} - ⁶H_{13/2} transitions (D₂O, 295K; λ_{exc} 270 nm); (lower) [Dy.L^{1a}] (dotted) and [Dy.L^{2a}(H₂O)] in a frozen MeOH/EtOH (4:1) glass at 80 K; note how the bands for [Dy.L^{1a/b}] at 494, 469, 460 and 589/582.5 nm at 295K either disappear or are x10 lower in intensity.

Table 1 Energies of transitions observed for [Dy.L^{1a}] and [Dy.L^{2a}(H₂O)] in solution (D₂O, 295 K, R = H) ^{a,b}

Complex	⁴ F _{9/2} -- ⁶ H _{15/2} energy/cm ⁻¹	⁴ F _{9/2} -- ⁶ H _{13/2}
[Dy.L ^{1a}]	20,242*(s)	16,978*(s)
	20,408	17,167*(s)
	20,620	17,331
	20,768	17,422
	20,920	17,559
	20,986	

2016 PCCP

	21,368*(w)	
	21,739*(w)	
[Dy.L ^{2a} (H ₂ O)]	20,555	17,180
	20,611	17,345
	20,812	17,390
	20,899	17,482
	21,008	17,575*(w)
	21,097	

^a Bands with an asterisk were absent or of much reduced intensity in a MeOH/EtOH (4:1) frozen glass at 80 K; ^b w = weak, s = strong.

Variable field relaxation studies

Measurements of the longitudinal relaxation rate of the reporter *t*-butyl proton signal in the dysprosium complexes were made at 295 K in D₂O, over the magnetic field range 1 to 16.5 T. Iterative minimisation methods were used, assuming classical BRW theory, to estimate values of μ_{eff} , τ_r and T_{1e} , holding the Ln-proton average distance, r , at 6.6 Å for each Dy complex examined within the series of ligands studied, (Tables 2 and 3). The selected value of r had earlier been shown to correspond to the average distance estimated using DFT calculations, based on consideration of closely related X-ray structural analyses.¹¹

Table 2 ¹H NMR shift and relaxation rate data for the C(CH₃)₃ resonance of [Dy.L¹] (295 K, D₂O, r 6.6 Å) to give the ‘best fit’, μ_{eff} , τ_r and T_{1e} values.

R	$\delta_{\text{H}}/\text{ppm}^{\text{a}}$	R_1/s^{-1}						$\mu_{\text{eff}}/\text{BM}^{\text{a}}$	T_{1e}/ps	τ_r/ps	R_1/R_2 9.4 T
		1.0 T	4.7 T	9.4 T	11.7 T	14.1 T	16.5 T				
H	-75	40±2	59±1	96±1	114±1	132±1	150±1	9.47(3)	0.45(2)	249(3)	0.59
N(CH ₃) ₂	-77	45±4	75±1	135±1	161±1	187±1	217±1	10.45(4)	0.42(4)	253(3)	0.56
SCH ₂ CO ₂ ⁻	-76	53±6	87±3	158±1	179±1	201±1	215±1	10.69(7)	0.44(5)	357(2) ^b	0.55
NO ₂	-81	45±3	66±1	109±1	129±1	150±1	168±1	9.78(4)	0.47(3)	259(3)	0.52
CONH ₂	-79	^c	63±1	110±3	131±1	151±1	170±1	9.82(4)	0.43(3)	262(3)	0.60
PO(OH)O ⁻	-76	54±5	88±3	156±1	179±1	195±1	218±1	10.65(6)	0.46(4)	345(3) ^d	0.50 ^e
Cl	-77	45±3	81±2	141±1	168±1	196±1	220±1	10.55(3)	0.41(3)	279(2)	0.70

^a the value of μ_{eff} for the free Dy(III) ion is usually considered to be 10.4 ± 5%; data beyond this range is given in bold.

^b for data fitted with a fixed τ_r = 280 ps, minimisation gave a poorer fit, with μ_{eff} = 10.58 BM, and T_{1e} = 0.50 ps. (ESI)

^c not determined as spectrum too weak

^d for data fitted with a fixed τ_r = 280 ps, minimisation gave a poorer fit: μ_{eff} = 10.56 BM, and T_{1e} = 0.51 ps. (ESI)

^e measured at pH 9 (R=P(O)₂, pK_a = 7.1 (295 K; I = 0)); at pH 7.1 exchange broadening increases T_2^* by a factor of 2.5.

Table 3 ^1H NMR shift and relaxation rate data for the $\text{C}(\text{CH}_3)_3$ resonance of $[\text{Dy}(\text{L})_2]$ (295 K, D_2O , r 6.6 Å) to give ‘best fit’ μ_{eff} , τ_r and T_{1e} values.

R	δ_{H} /ppm	R_1/s^{-1}						$\mu_{\text{eff}}/\text{BM}^{\text{a}}$	T_{1e}/ps	τ_r/ps	R_1/R_2 9.4T
		1.0 T	4.7 T	9.4 T	11.7 T	14.1 T	16.5 T				
H	-21	55±2	73±1	124±1	149±1	170±1	210±2	10.32(2)	0.52(2)	196(3)	0.56
$\text{N}(\text{CH}_3)_2$	-28	52±4	83±1	144±2	168±1	198±1	223±1	10.55(4)	0.47(3)	267(4)	0.60
$\text{SCH}_2\text{CO}_2^-$	-18	59±1	99±1	181±1	219±1	259±1	297±1	11.36(1)^b	0.46(1)	248(1)	0.60
NHCOCH_3	-23	53±5	85±1	152±2	180±1	210±1	241±1	10.75(5)	0.46(4)	258(4)	0.61
NO_2	-28	59±3	88±2	149±1	175±1	199±1	224±1	10.57(3)	0.52(3)	285(3)	0.46

^a the value of μ_{eff} for the free Dy(III) ion is usually $10.4 \pm 5\%$; data beyond this range is given in **bold**.

^b for data fitted with fixed $\tau_r = 357$ ps (as for the analogous $[\text{Dy}(\text{L})_1]$ complex), minimisation did not fit the data well, and gave $\mu_{\text{eff}} = 11.5$ BM (i.e. even higher), and $T_{1e} = 0.35$ ps, values that are out of line with the other analyses (see ESI)

The fits to equation (1) of the sets of experimental data for each example converged to well-defined minima, (Tables 2 and 3, Figure 2 and ESI). R_2 data were also determined from resonance linewidths (ESI) but these were not used to fit BRW equations due to the large errors in these values ($\pm 10\%$). The ratio of R_1/R_2 (which is an important parameter for imaging) in Tables 2 and 3, at 9.4 T, varies by only $\pm 20\%$ in each system, as the *para*-substituent is changed. Thus, the R_2 rates of relaxation follow a similar dependence on the substituent as the R_1 rates.

For each series of complex, the fitted values of T_{1e} converged uniformly to 0.46 (± 0.06) ps, consistent with the similar values for R_1 measured at 1 Tesla. Given that the electronic relaxation time is believed to be proportional to the size of the transient ligand field induced by solvent collision, the common value accords with the absence of change in the overall ligand field observed by optical spectroscopy.

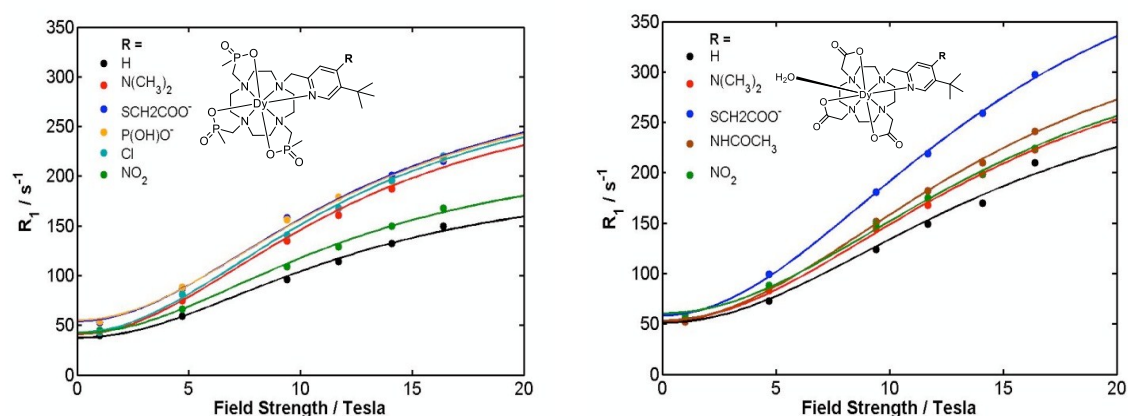


Figure 2 ^1H NMR relaxation rates (R_1/s^{-1}) for the *t*Bu resonances in $[\text{Ln}(\text{L})_1]$ (left) and $[\text{Ln}(\text{L})_2(\text{H}_2\text{O})]$ (right) as a function of magnetic field, showing the fits (line) to the experimental data points (295 K, D_2O).

2016 PCCP

The longitudinal relaxation rates tend to diverge to higher values at high field for the anionic *para*-substituents (R= SCH₂COO⁻ or P(OH)O⁻), with respect to the parent complex (R = H) in each system, with a 43% increase in R_1 at 16.5 T from [Dy.L^{1a}] to [Dy.L^{1f}], and a 41% increase from [Dy.L^{2a}] to [Dy.L^{2d}]. In the [Dy.L²] series, this results in an unusually high estimated value of μ_{eff} for [Dy.L^{2e}] of 11.4 BM, fitted with standard BRW theory using a fixed value of $r = 6.6 \text{ \AA}$. For the [Dy.L¹] series, it is the fast relaxing (at high field) systems which minimised to the expected μ_{eff} for free Dy(III) ions, $\mu_{\text{eff}} = ca. 10.6 \text{ BM}$, whereas the set of more slowly relaxing complexes, (R = H, NO₂, CONH₂), gave rise to an unusually low μ_{eff} value of 9.5 to 9.8 BM.

The estimated values of μ_{eff} thus showed a significant variation, beyond the $\pm 5\%$ range, and these deviations echo the significant change in R_1 values measured at high field, where the size of μ_{eff} has its greatest impact on the relaxation rate, assuming BRW theory. The pair of anionic complexes in the [Dy.L¹] series gave rise to the largest estimated value for τ_r , consistent with the large apparent molecular volume of a strongly hydrated anion.

The variation in the estimated τ_r values does not correlate with the steric bulk of the substituent *ortho* to the *t*-butyl group, as defined by their relative 'A' values or data for closely related substituent groups, (Cl, 2.4; CONH₂, 5.0; NO₂, 4.8; SMe, 4.3; SO₂Me, 10.5; NMe₂, 8.8; CO₂H 5.9)) suggesting that a steric effect, restricting the local motion of the tertiary butyl group, is not likely to be significant here.

Table 4 ¹H NMR shift and relaxation rate data for the three P(CH₃) resonances of [Dy.L¹], R=NO₂, SCH₂COO⁻ (295 K, D₂O), to give the 'best fit' μ_{eff} , τ_r and T_{1e} values, fixing $r = 4.6 \text{ \AA}$.

R=	¹ H	$\delta_{\text{H}}/\text{ppm}^{\text{a}}$	R_1/s^{-1}						$\mu_{\text{eff}}/\text{BM}$	T_{1e}/ps	τ_r/ps
			1.0 T	4.7 T	9.4 T	11.7 T	14.1 T	16.5 T			
NO ₂	P(CH ₃)	+70	410±30	640±30	1230±10	1380±20	1640±20	1870±20	10.44(4)	0.42(3)	268(2)
NO ₂	P(CH ₃)'	+100	- ^a	770±30	1410±20	1580±40	1820±30	2030±40	10.75(4)	0.46(3)	312(2)
NO ₂	P(CH ₃)''	+103	- ^a	500±20	890±10	1070±20	1250±10	1390±10	9.68(3)	0.39(1)	261(2)
SCH ₂ CO ₂ ⁻	P(CH ₃)	+52	350±50	690±50	1200±20	1390±30	1560±10	1730±20	10.41(6)	0.37(5)	344(1)
SCH ₂ CO ₂ ⁻	P(CH ₃)'	+99	560±50	850±30	1400±30	1520±20	1720±20	1810±20	10.62(8)	0.55(4)	380(5)
SCH ₂ CO ₂ ⁻	P(CH ₃)''	+90	320±20	570±30	900±10	1060±10	1170±10	1280±10	9.60(5)	0.40(3)	344(2)

^a not determined due to overlapping P(CH₃)' and P(CH₃)'' resonances. Average R_1 for the overlapped peak = 410±90 s⁻¹.

The three methyl phosphinate proton resonances of two [Dy.L¹] complexes were also investigated in order to garner further information regarding the anisotropy of the Curie relaxation term. Longitudinal relaxation rates of the three P-methyl groups were fitted using the BRW equation (1), holding the Ln-proton average distance, r , at 4.6 \AA . based on analyses of closely related structures (Table 4 and ESI). Notably, data for the nitro-substituted [Dy.L¹] complex minimised to the equation *a priori*, without fixing the distance r , with every P-

2016 PCCP

methyl group fitting well for $r = 4.6 \pm 0.1 \text{ \AA}$.

The data in Table 4 reveal that for each complex, the three P(CH₃) proton groups relax at significantly different rates, notwithstanding their likely similar distances from the paramagnetic centre, r . In each case, the T_{1e} values are very similar, whichever proton signal is used in the relaxation analysis ($\pm 10\%$). In addition, the value of τ_r varies by only $\pm 20\%$, thus the rotational motion does not appear to be significantly anisotropic in either case. Therefore, it would seem that the calculated values of μ_{eff} for a given complex apparently vary, according to whichever PMe or *t*Bu resonance is examined. Clearly this cannot be the case, and the analysis requires that the anisotropy of the magnetic susceptibility tensor be explicitly considered.

The relaxation rates of each different P(CH₃) group are similar in the two complexes up to 9.4 T, and then diverge, with [Dy.L¹] (R=SCH₂CO₂⁻), having rates *ca.* 10% lower at 16.5 T. This is the opposite behaviour to that observed with the *t*-butyl resonance (30% increase at 16.5 T) (Table 2). Such behaviour lends support to the premise that the rate is not affected by the nature and motional dynamics of the substituent group, but rather is sensitive to the angle of the proton in question with respect to the major magnetic susceptibility axes

Summary and Conclusions

In standard BRW theory, the Curie relaxation term is usually considered to arise from rotational modulation of the dipolar interaction between the nucleus and the time-averaged electron magnetic dipole moment induced in the electron shell by the applied magnetic field. The point dipole moment approximation is used because it is assumed that the f orbitals are localised very close to the metal. This analysis gives rise to a fourth power dependence of the relaxation rate on the size of the average magnetic susceptibility, μ_{eff} .

The anisotropy of the magnetic susceptibility tensor has been explicitly considered theoretically by Vega and Fiat, and leads to a modification of equation (1), to give equation (2)^{1b,1c}. Consideration has been given in the past to the preferred use of an experimental value for the magnetic susceptibility, rather than a calculated value for μ_{eff} . No examples appear to have been published of either of these approaches being used to analyse field-dependent relaxation rate data.

The studies in this work reveal how small changes to the polarisability of one pyridine donor, both in 8 and 9-coordinate systems, can have pronounced consequences on experimental nuclear relaxation rates, with changes of the order of 50% evident in each series examined.

2016 PCCP

$$R_1 = -4F \frac{3\tau_r}{1 + 9w_N \tau_r^2} + 4F^1 \frac{\tau_r}{1 + w_N^2 \tau_r^2}$$

where $F = -\frac{3}{8} \left(\frac{1}{4\pi} \right)^2 \frac{w_N^2 \varepsilon}{r^6}$

$$F^1 = \frac{3}{10} \left(\frac{1}{4\pi} \right)^2 \frac{w_N^2}{r^6} \left[\chi^2 + 4\pi r^3 \chi \delta^{pcs} - \frac{\varepsilon}{4} + \left(\chi_{xx}^2 + \chi_{yy}^2 + \chi_{zz}^2 - 3\chi^2 \right) / 6 \right]$$

$$\varepsilon = \frac{x^2 y^2 (\chi_{xx} - \chi_{yy})^2 + x^2 z^2 (\chi_{xx} - \chi_{zz})^2 + y^2 z^2 (\chi_{yy} - \chi_{zz})^2}{r^4} \quad (2)$$

The changes did not correspond to obvious differences in the ${}^6\text{H}_{15/2}$ electronic energy levels, as revealed by optical spectroscopy. The splitting of the ligand field was independent of the nature of the pyridine substituent, in accord with the similar relaxation rates measured at 1 T, and the constant electronic relaxation rates, T_{1e} , estimated in every case. By analysing different reporter proton resonances in the same complex and using classical BRW theory, variable values of μ_{eff} were estimated yet with similar ‘best-fit’ values for T_{1e} and τ_r . Such findings support the premise that relaxation rate data analyses must be assessed with appropriate allowance for the angular position of the reporter group, with respect to the major magnetic susceptibility axes.

Relaxation rate/structural correlations are important issues for the design of paramagnetic shift (PARASHIFT) agents for MR imaging⁹⁻¹¹, where functionalization of molecular probes (judiciously designed to optimize chemical shift *and* nuclear relaxation rates for imaging) to allow targeted and/or ‘smart’ imaging, may have significant effects upon relaxation rates, relative to the parent probe structure.

Overall, the findings here lend support to the notion that our interpretation of the theory of paramagnetic relaxation requires a more intuitive understanding to be developed between ligand structural variation, lanthanide ion permutation and relaxation behaviour. The *anisotropy* of the ligand field is surprisingly sensitive to remote ligand substitution and evidently has a significant impact in systems of low symmetry, via the differing contributions of the lowest energy $|m_J|$ states to the size and the anisotropy of the magnetic susceptibility tensor.^{1b, 13} Further low temperature EPR and magnetic susceptibility measurements are required, seeking to explore these aspects in greater detail.

Acknowledgement We thank the ERC (FCC 266804) and EPSRC for support.

2016 PCCP

§ Supplementary information is available: relaxation rate data analyses under differing boundary conditions, additional emission spectra, representative complex characterisation and a discussion of error analyses.

Notes and References

1. a) A.G. Redfield, *IBM Journal of Research and Development*, 1957, 1, 19-31; b) I. Bertini, C. Luchinat and G. Parigi, *Prog. Nucl. Mag. Reson. Spectrosc.* 2002, **40**, 249-273; c) A. J. Vega and D. Fiat, *Mol. Phys.* 1976, **31**, 347.
2. A. M. Funk, P. Fries, A. M. Kenwright, P. Harvey and D. Parker, *J. Phys. Chem. A*, 2013, **117**, 905-917; values of T_{1c} for Gd(III) analogues are about three to four orders of magnitude bigger.
3. a) J. Jensen, A. R. Mackintosh, *Rare Earth Magnetism*; International Series of Monographs of Physics; Clarendon Press: Oxford, 1991; b) H. Curzen, L. Bovigny, C. Bulloni and C. Daul, *Chem. Phys. Letts.* 2013, **574**, 129-132.
4. a) A. S. Souza, M. A. Couto dos Santos, *Chem. Phys. Lett.* 2012, **521**, 138-141; b) V. S. Mironov, Y. G. Galyametdinov, A. Ceulemans, C. Görrler-Walrand, K. Binnemans, *J. Chem. Phys.* 2002, **116**, 4673-4685.
5. C. Görrler-Walrand and K. Binnemans in *Handbook on the Physics and Chemistry of Rare Earths*; K. A. Gschneidner and L. Eyring, eds. Elsevier, 1996; vol. 23, pp. 121-283.
6. C.-G. Ma, M. G. Brik, V. Kiisk, T. Kangur, I. J. Sildos, *J. Alloys Compd.* 2011, **509**, 3441-3451; F. Auzel, O. L. Malta, *J. Phys.* 1983, **44**, 201; O. L. Malta, E. Antic-Fidancev, M. Lemaitre-Blaise, A. Milicic-Tang, M. Taibi, *J. Alloys Compd.* 1995, **228**, 41.
7. J. Holsa, M. Lastusaari, J. Niittykoski, R. S. Puche, *Phys.Chem.Chem.Phys.* 2002, **4**, 3091-8.
8. J. D. Rinehart and J. R. Long, *Chem. Sci.*, 2011, **2**, 2078; J. Luzon and R. Sessoli, *Dalton Trans.* 2012, **41**, 13556.
9. P. Harvey, A. M. Blamire, J. I. Wilson, K-L. N. A. Finney, A. M. Funk, P. K. Senanayake, D. Parker, *Chem. Sci.* 2013, **4**, 4251.
10. A. M. Funk, K-L. N. A. Finney, P. Harvey, A. M. Kenwright, E. R. Neil, N. J. Rogers, P. K. Senanayake and D. Parker, *Chem. Sci.* 2015, **6**, 1655.
11. A. M. Funk, P. Harvey, K-L. N. A. Finney, M. A. Fox, A. M. Kenwright, N. J. Rogers, P. K. Senanayake and D. Parker, *Phys. Chem. Chem. Phys.* 2015, **17**, 16507.
12. a) M.-E. Boulon, G. Cucinotta, J. Luzon, C. Degl'Innocenti, M. Perfetti, K. Bernot, G. Calvez, A. Caneschi and R. Sessoli, *Angew. Chem. Int. Ed. Engl.* 2013, **52**, 350; b) G. Cucinotta, M. Perfetti, J. Luzon, P. E. Car, A. Caneschi, G. Calvez, K. Bernot and R. Sessoli, *Angew. Chem. Int. Ed. Engl.* 2012, **51**, 1606.
13. O. A. Blackburn, N. F. Chilton, K. Keller, C. E. Tait, W. K. Myers, E. J. McInnes, A. M. Kenwright, P. D. Beer, C. R. Timmel, S. Faulkner, *Angew. Chem. Int. Ed. Engl.* 2015, **54**, 10783.
14. R. S. Dickins, D. Parker, J. I. Bruce and D. J. Tozer, *Dalton Trans.* 2003, 1264.

2016 PCCP

15. S. Shintoyo, K. Murakami, T. Fujinami, N. Matsumoto, N. Mochida, T. Ishida, Y. Sunatsuki, M. Watanabe, M. Tsuchimoto, J. Mrozinski, C. Coletti and N. Re, *Inorg. Chem.* 2014, **53**, 102 359.
16. J. Long, V. Remi, R. A. S. Ferreira, L. D. Carlos, F. A. A. Paz, Y. Guari and J. Larionova, *Chem. Commun.* 2012, **48**, 9974.